**Thirteenth International Conference of Fluid Dynamics**
**21-22 December, 2018, Steigenberger Hotel El Tahrir, Cairo, EGYPT**

**ICFD13-EG-6073**

# URANS and LES Simulations of Transient Combustion of Turbulent Premixed Hydrogen-Air Mixtures Using Flamelet Surface Models

**Mohamed A. Yehia, Hatem O. Haridy and Fawzy Abdel Aziz**
Department of Mechanical Power, Faculty of Engineering, Cairo University, Giza Egypt

**ABSTRACT**
The complex phenomena associated with the explosion of a flammable mixture of hydrogen-air still poses challenges to the scientific community. Modelling various variables affecting the reacting turbulent flow represents the foundation that is complemented by sound numerical algorithms. The immediate consequences of igniting such mixture in a semi-confined geometrical configuration is numerically examined. In this study, focus will be devoted to the assessment of the extra benefits brought about by using LES, rather than URANS modelling techniques. The well-established flamelet model based on solving transportation equations for 'flame surface density' is here further developed by a Dynamic Flame Surface Density model 'DFSD', to be incorporated in an in-house code 'PUFFIN' of Loughborough University that involves Large Eddy Simulations 'LES' techniques. The model is examined through comparison with valuable and reliable laser measurements obtained for different turbulence levels in Sydney University. The performance is also compared with results obtained from the commercial code ANSYS FLUENT[1], with Unsteady Reynolds Averaged Navier-Stokes model with the standard k-ε model modified for compressible flows and the extended coherent flame model. Results include demonstration of the ability of the two models to reproduce similar values for over-pressure history and flame position to the various sets of experiments available for the hydrogen-air mixture. The models succeeded in capturing the mean features of the flow, with some discrepancies more evident in the less turbulent cases.

**KEYWORDS:**
Large eddy simulations-Turbulent premixed combustion-Equivalence ratio.

## INTRODUCTION

It is hard to imagine that the traditional diesel and petrol internal combustion engines would successfully pass through the waves of modernization that are currently changing all our ways of life, as the main driver to our automotive industry around the world. The call for higher specific power, lower pollution emissions has been the goal for development and research for too long. The idea of burning liquid fossil fuel and pouring the combustion products directly into populated streets to be inhaled into human lungs is getting less attractive and less consistent with modern means of life. Alternatives being currently considered include electricity and/or the use of hydrogen as a fuel, with its attractive exclusive property of producing the number one human friendly matter as its only combustion product: $H_2O$.

However, hydrogen, unlike presently used fuels, is not a natural resource that is found on earth at no cost other than mining, refining and transporting. It has to be manufactured at a cost that puts it at a disadvantageous comparison with fossil fuels, which are still the most economical means and certainly the current source of around 98% of the hydrogen produced around the world. Electro-lysing of water is still expensive, and it would then make more sense to directly use the electricity in empowering electric motors to move automotives. Beside the costs, the high reactivity of hydrogen poses another subject that still requires a thorough understanding before introducing networks of that gas all around the globe.

The intended or accidental burning of hydrogen would usually occur on turbulent premixed form. In spite of continuous effort in experimental and mathematical research,[2], complexities associated with the inter-related phenomena have not yet been resolved.

 

Computational Fluid Dynamics, CFD codes which delivered closure to plenty of engineering problems did not come yet to conclusion when it comes to such problems as the flame propagation in a turbulent premixed environment.
Today CFD has become a widely known approach to address many engineering challenges. The last two decades has seen a significant growth in affordable computer hardware which in turn has allowed large complex engineering problems to be simulated. Typically today it is possible to find companies dealing with 1 billion cells. The basis of CFD forms from the Navier-Stokes Equations (NSE). While it is known that accurate simulation results can be obtained with Direct Numerical Simulation (DNS) and Large Eddy Simulation (LES) of the NSE, such approaches require fine grids and time resolutions requiring unfeasible amount of memory and calculation times. Furthermore, DNS and LES still have their inherent areas that still require more research, such as robust solver development, modelling sub-grid scales, and handling large data. To date, Reynolds Averaged Navier-Stokes (RANS) equations form the dominant approach for solving many engineering problems encountered around the world.
To date, no global models are available to satisfy all the regimes of combustion but models are developed for certain regimes. These regimes define the mode of combustion based on flame and turbulence characteristics. Peters [3] defines wrinkled flamelets, corrugated flamelets, thin reaction zone, and broken reaction zone based on the Karlovitz number, and normalised turbulence intensity and length scale. Many practical applications operate in the thin reaction, corrugated, and wrinkled zones and there has been considerable effort in modelling turbulent premixed flames in these regimes. For turbulent premixed combustion several models are available, such as, the Bray-Moss-Libby (BML) model, which models the mean rate of reaction using an algebraic expression for the flame surface density; the Eddy-Dissipation model, which assumes that mixing controls the rate of reaction; the Coherent Flame Model (CFM), which solves a transport equation for the flame surface density; or the Zimont model [4], which models the turbulent burning velocity. In this paper the focus will be on the CFM model which is available in the commercial Fluent and PUFFIN CFD codes.
Validation of the models is a critical task to enable solving real engineering problems since it provides an indication of the models ability to predict accurately.
One of the sources of ambiguity in the field of flame propagation in a turbulent premixed flammable mixture is the very fact of the presence of plenty of experimental and numerical efforts. Examples can be reviewed in [5]–[19]. It might be always useful to provide higher resolution and more accurate and reliable experimental data. As for the efforts to simulate the available data with the aid of CFD models, the range at which the satisfactory validation exercise can be extended to various sets of experiments is still questionable.
The coherent flame model for turbulent chemical reaction has originally been proposed by [20]. It suggests that the flame structure is composed of a distribution of flame elements, whose thickness is much smaller than the large turbulent eddies. The flame elements, later named laminar flamelets are strained due to gas motion and annihilated due to reaction consumption. The coherent flamelet model (CFM) [20] is based on the concept that the mean chemical reaction rate per unit volume is the product of two quantities: the reaction rate per unit area of the flamelets and the average flamelet area per unit volume. The first quantity is assumed to be proportional to the laminar burning velocity; the second quantity is the flame surface density. The model assumes that the flow field is separated by the flame sheet to the reactants and the products. This sheet becomes extensively wrinkled, distorted and dispersed during the turbulent process and thus the variable $\Sigma(x_i,t)$ which specifies the flame surface density has been introduced.
In the present study, a detailed comparison would be given between experimental data produced by the Sydney University, Australia [7], [21], [22] and predictions for the same cases using the well-known commercial code ANSYS FLUENT applying RANS analysis, and PUFFIN which is the code written by Loughborough University, United Kingdom applying LES with Dynamic Flame Surface Density, DFSD on the Sub-Grid Scale, SGS. The latter has originally been formulated by [23], and further developed by [24], and has been used to predict similar cases to those mentioned in the present study in [8], [18], [25]. Though PUFFIN and its Loughborough University 'ancestors' have previously been used to numerically investigate and elucidate the Sydney University experimental data, this present study is considered amongst the earliest in applying the famous and widely accepted FLUENT to the same set of data. This study would certainly be followed by more rigorous ones to verify the available built in models to examine the turbulence-chemistry interaction against the same set of experimental data.
The turbulent flame can be considered as an ensemble of locally stretched laminar flames, called flamelets. The turbulence and chemical reaction interact with each other, where the flow field of the flame front is affected on both the burnt and unburnt sides of the flame. The eddies produced by turbulence convect and distort the flame front. In flamelet approaches, flame position is tracked through iso-c (progress variable) surfaces for premixed flames.
LES explicitly resolves the large-scale unsteady motions that are known to play a significant role when the reactants are premixed, while the smaller eddies are modelled.

## THE COMBUSION CHAMBER

The cases under consideration here involve the University of Sydney combustion chamber used which is of volume of 0.625L having a square cross-section of 50 mm and a length of 250 mm as shown in Figure 1. Details of the chamber configuration and measuring instruments can be found in [26]. The combustion chamber consists of three exchangeable solid baffle plates each of square configuration of dimensions 50 mm x 50 mm and thickness of 3 mm. This consists of five 4 mm wide bars each with a 5 mm wide space separating them, rendering a blockage

 

ratio of 40%. The baffle plates are aligned at 90 degrees to the solid. The number of plates inserted in the flow allows for different blockages to the flow and thus different levels of turbulence to the flow. This chamber is of particular interest because of its smaller volume and potential to hold a flame propagating in strong turbulence.

These baffle plates are denoted as B1, B2 and B3. They are located at 20, 50 and 80 mm respectively from the ignition point. The combustion chamber has a built-in solid square obstacle of 12mm in cross-section, which is centrally located at 96 mm from the ignition point running throughout the chamber cross-section, which causes significant formation to the flow turbulent eddies. The pressure is measured using Piezo-resistive pressure transducers with a range of 0–1bar and a response time of 0.1ms. The pressure transducer is positioned at the ignition end of the combustion chamber. The exact location is on the central plane of x-axis, 37 and 5 mm on y and z axis respectively from the left bottom of the chamber.

In the present study, the cases considered involve a Hydrogen air mixture of equivalence ratio of 0.7, with the details of baffles inside the chamber changed from one case to the other so that case one is BBBS, similar to that shown in Fig 1a, while the following three cases BB0S, B00S and 000S are configured according to number and location of baffles. The configurations are symbolized according to the baffles and obstacle as, the baffle by (B), the solid obstacle by (S), and location with no baffles or obstacle by (0).

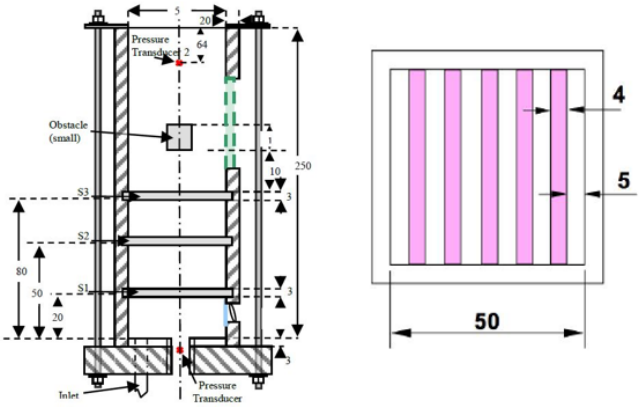


Figure 1: (a) cross section of the combustion chamber (b) dimensions of the baffle plates. All dimensions are in mm

## MODELLING AND NUMERICAL APPROACH

Turbulent combustion is basically a reacting flow combined with heat transfer, chemistry and fluid flow. Therefore, in addition to mass, momentum and energy conservation equations, species conservation should be closed then solved in order to simulate the combustion phenomena. In this study two mathematical facilities have been used. The commercial code ANSYS Fluent [1] is used as a numerical tool and the finite volume method is employed to solve the Unsteady Reynolds Averaged Navier-Stokes (URANS) equations which are given as follows:

Mass and momentum conservation equations;

$$\frac{\partial \rho}{\partial t} + \frac{\partial (\rho u_j)}{\partial x_j} = 0 \quad (1)$$

$$\frac{\partial \rho u_i}{\partial t} + \frac{\partial (\rho u_i u_j)}{\partial x_j} = -\frac{\partial P}{\partial x_i} + \frac{\partial}{\partial x_j}\left(2\mu\left[S_{ij} - \frac{1}{3}\delta_{ij}S_{kk}\right]\right) \quad (2)$$

Where $u_i$ is the velocity component in $i$ direction (m/s), P is pressure (kPa), $\rho$ is density $(m^3/kg)$, $\mu$ is dynamic viscosity $(N.S/m^2)$, and $S_{ij}$ is the strain rate which is expressed as,

$$S_{ij} = \frac{1}{2}\left(\frac{\partial u_i}{\partial x_j} + \frac{\partial u_j}{\partial x_i}\right) \quad (3)$$

And the energy equation can be expressed in terms of enthalpy, $h$ as:

$$\frac{\partial \rho h}{\partial t} + \frac{\partial (\rho u_j h)}{\partial x_j} = \frac{\partial P}{\partial t} + 2\mu\left[S_{ij} - \frac{1}{3}\delta_{ij}S_{kk}\right]\frac{\partial u_j}{\partial x_i} + \frac{\partial}{\partial x_j}\left(\frac{\mu}{Pr}\frac{\partial h}{\partial x_j}\right) + \dot{q_c} \quad (4)$$

Contributions due to pressure work, viscous dissipation, and flow dilatation are represented by the first three terms on the right hand side. The last term in equation is the chemical source term, which, for a premixed flame given by:

$$\dot{q_c} = \Delta h_f^{\circ} \dot{\omega}_c Y_{fu}^{\circ} \quad (5)$$

The standard k-ε model [27] is used to predict the turbulence in the flow. The transport equations for the turbulent kinetic energy
k and its dissipation ε are as follows [

$$\frac{\partial (\rho k u_i)}{\partial x_i} = \frac{\partial}{\partial x_i}\left[\left(\mu + \frac{\mu_t}{\sigma_k}\right)\frac{\partial k}{\partial x_i}\right] + \Gamma - \rho\varepsilon \quad (6)$$

$$\frac{\partial (\rho \varepsilon u_i)}{\partial x_i} = \frac{\partial}{\partial x_i}\left[\left(\mu + \frac{\mu_t}{\sigma_\varepsilon}\right)\frac{\partial \varepsilon}{\partial x_i}\right] + C_1\Gamma\varepsilon - C_2\frac{\varepsilon^2}{k+\sqrt{\nu\varepsilon}} \quad (7)$$

$$\Gamma = -\overline{u_i u_j}\frac{\partial u_i}{\partial x_j} = \frac{\mu_t}{\rho}\left(\frac{\partial u_i}{\partial x_j} + \frac{\partial u_j}{\partial x_i}\right)\frac{\partial u_i}{\partial x_j} \quad (8)$$

$$\mu_t = \rho C_\mu \frac{k^2}{\varepsilon} \quad (9)$$

$$C_1 = max\left[0.43, \frac{\mu_t}{\mu_{t+5}}\right] \quad (10)$$

The rest of the constants are taken to be;

$C_2 = 1.0$
$\sigma_k = 1.0$
$\sigma_\varepsilon = 1.2$

The LES mathematical model used here is the Loughborough University PUFFIN which involves a sub-grid scale model following the Smagronisky principle [28]. The flame surface density model used to model combustion is described in a twin study [29]. It is modified to a so called Dynamic Flame Surface

Density Model (DFSD). The inner cut-off scale equals three times the laminar flame thickness, where the same value was used [23] and it proved being able to predict good results from experimental extractions.
A dynamic procedure [30] was developed to calculate the model coefficient from local instantaneous flow conditions. In this procedure, test filter is used and applied to the filtered Navier-Stokes equation. Application of the test filter, which is larger than the grid filter, allows extracting information from the smallest resolved scales. This model was extended to compressible flows,[30] which is used in the present simulations. The Leonard stresses, which represents the contribution of the Reynolds stresses of scales with length lies between the test and grid filter width. Leonard stresses can be expressed using the known Germano identity[30]:

$$L_{ij} = T_{ij} - \tau_{ij}^{sgs} \quad (11)$$

Where $T_{ij}$ and $\tau_{ij}^{sgs}$ are the sub-grid scale stresses at the test and grid levels respectively. A scalar equation of the model coefficient can be written as:

$$C(y,t) = \frac{(L_{ij}^{a}\tilde{S}_{ij})_y}{(\bar{\beta}_{ij}\tilde{S}_{ij} - \alpha_{ij}\tilde{S}_{ij})_y} \quad (12)$$

And the traceless tensors $\beta_{ij}$, $\alpha_{ij}$ are:

$$\beta_{ij} = -2\bar{\rho}C\bar{\Delta}^2\left|\tilde{S}\right|(\tilde{S}_{ij} - \tfrac{1}{3}\delta_{ij}\tilde{S}_{kk}) \quad (13)$$

$$\alpha_{ij} = -2\bar{\rho}C\hat{\Delta}^2\left|\hat{\tilde{S}}\right|(\hat{\tilde{S}}_{ij} - \tfrac{1}{3}\delta_{ij}\hat{\tilde{S}}_{kk}) \quad (14)$$

The above equations are modified by Libby who proposed a tensor $M_{ij}$ instead of $S_{ij}$ therefore, the model coefficient is written as:

$$C = \frac{\mathcal{L}_{ij}M_{ij} - \frac{1}{3}\mathcal{L}_{ll}M_{mm}m}{2\bar{\Delta}^2(M_{ij}M_{ij} - \frac{1}{3}M_{ll}M_{mm})} \quad (15)$$

$$\text{While } M_{ij} = (\widehat{\bar{\Delta}}/\bar{\Delta})^2\hat{\bar{\rho}}\left|\hat{\tilde{S}}\right|\hat{\tilde{S}}_{ij} - \bar{\rho}\widehat{\left|\tilde{S}\right|\tilde{S}_{ij}} \quad (16)$$

Hence, the Smagorinsky model coefficient can be calculated at each spatial grid location and time by the dynamic procedure.
A relation was proposed between the inner cut-off scale and laminar flame thickness according to DNS data [31] as follows:

$$\delta_c = \delta_l(\alpha_3 Ka^{\beta_3}) \quad (17)$$

In the above equation $Ka$ is the Karlovitz number, while $\alpha$ and $\beta$ are model constants. This equation is applicable for $u'/u_L$ values between 0.5 and 6.2. Since the value of $u'/u_L$ can reach 13.4 [31], the above equation may not be useful to define appropriate inner cut-off scale. In the present work the inner cut-off scale equals three times the laminar flame thickness, where the same value was used [31]and it proved being able to predict good results from experimental extractions.
For transient applications, ANSYS Fluent offers the possibility to use the fully implicit pressure based coupled solver (PBCS) or the density based (DBS) solver which has implicit and explicit options. A second order upwind scheme is used for the spatial discretization of all variables and second order implicit scheme is employed for the temporal discretization.
The first short ignition phase is not modeled in this simulation, since the ignition phase requires the solution of the Navier-Stokes equations with detailed chemistry. We use a simple ignition model described as follow: a small region in the domain at the spark location is patched with the progress variable c = 1. The ignition radius of 1 cm has been used and any small changes in the ignition radius lead only to some time shift of the results [32] with no consequence on the combustion physics. The stretch effects on the flame propagation, the preferential diffusion and the dynamic instability were not considered in our investigation. In addition the counter-gradient transport has a negligible influence on the results. In the CFM model, the flame front position has been obtained from the axial coordinate corresponding to an iso-surface value c= 0.5. At this location, the temperature is approximately 900 K and this value has been chosen the track the flame front in the CFM model.

The LES model used here solves strongly coupled Favre filtered flow equations outlined above, which are written in a boundary fitted coordinates and discretized by using a finite volume method. The spatial discretization is done with finite volume method on a non-uniform staggered Cartesian grid. Second-order central difference is used for discretization of diffusion, advection, and pressure gradient terms in the momentum equation, while the third order QUICK scheme is used in the regions outside the chamber where the accuracy is less important. Second order central difference is also used for the pressure correction equation and diffusion terms in the scalar equations, whereas SHARP technique is used for advection terms. The fractional step method is used to advance all the equations in time.

The equations are advanced in time using the fractional step method. Crank Nicolson scheme is used for the time integration of momentum and scalar equations. A number of iterations are required at every time step owing to strong coupling of equations with one other. Solid boundary conditions are applied at the bottom, vertical walls, for baffles and obstacle, with the power-law wall function used to calculate wall shear. Outflow boundary conditions are applied at the vented end of chamber. A non-reflecting boundary condition similar to commonly used convective boundary condition, in incompressible LES is used to avoid reflection of pressure waves at this boundary. The initial conditions are quiescent with zero velocity and reaction progress variable. Ignition is modelled by setting the reaction progress variable to 0.5 within a definite radius at the bottom center of the chamber.
The equations are solved using a Bi-Conjugate Gradient solver with an MSI pre-conditioner for the momentum, scalar and pressure correction equations. The time step is limited to ensure the CFL number remains less than 0.5 with the extra condition that the upper limit for $\delta t$ is 0.3 ms. The solution for each time step requires around 8 iterations to converge, with residuals for

 

the momentum equations less than 2.5e-5 and scalar equations less than 2.0e-3. The mass conservation error is less than 5.0e-8. Simulations were carried using a three dimensional, non-uniform, Cartesian co-ordinate system for compressible flow with low Mach number. Since this type of flow involves large changes in density, high velocities and significant dilatation, all terms in the governing equations are retained.

## THE COMPUTATIONAL DOMAIN

In order to simulate the turbulent premixed flame of the hydrogen/air mixture, a computational domain with initial and boundary conditions is required. The domain must extend in the direction normal to the outflow boundary to avoid any possible pressure reflections. However, to avoid certain numerical instabilities, in general, the domain is extended outside the combustion chamber.

A typical computational domain, superimposed with the numerical combustion chamber and obstacles is shown for clarity in Figures 2 and 3. The combustion chamber has dimensions of 50 x 50 x 250 mm. The flame propagates over the turbulence generating baffles and solid obstacle surrounded by solid wall boundary conditions. To ensure that the pressure wave leaves the chamber smoothly, without reflections, the open end of the domain is extended to 250 mm in the $z$ -direction with a far-field boundary condition. Similarly, the domain is extended to 325 mm in the $x$ and $y$ directions with large expansion ratios approximately equal to 1.25 outside the combustion chamber. The numerical model has been employed with a computational grid of 90×90×336 (2.7 million) cells in 3 dimensional space. It should be noted that any further grid refinement beyond this grid has no significant impact on the results [22], [25].

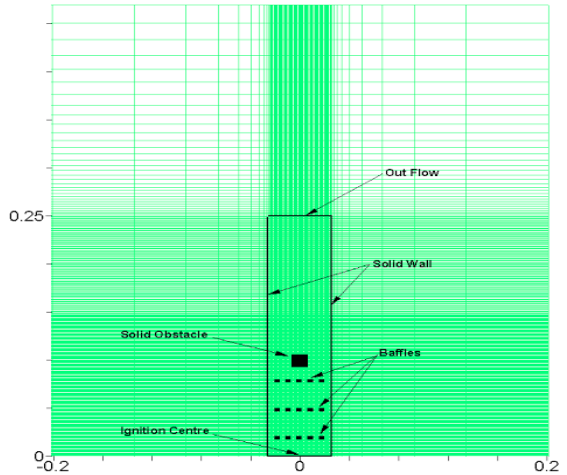


Figure 2: The Computational Domain of the Combustion Chamber

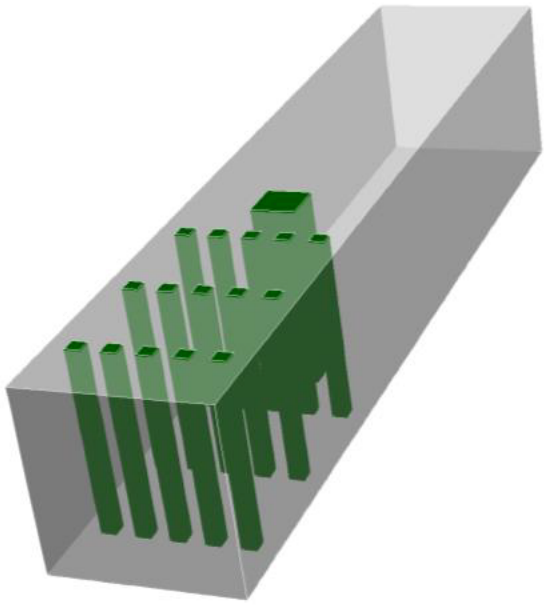

Figure 3: Schematic diagram of the flow configuration.

## RESULTS AND DISCUSSION

The base configuration has three baffle plates and small square obstacle of 12 mm in cross section. The plates and the obstacle are rendering a blockage ratio of 40% and 24% respectively. For simplicity, this configuration is labeled as “BBBS”. Figure 4 demonstrates the measured change of pressure and flame position with time as obtained by [7] and as predicted by the two modelling techniques namely Unsteady Reynolds Averaged Navier Stokes (URANS) utilizing FLUENT and Large Eddy Simulations (LES) utilizing PUFFIN for the four different configurations of the Sydney University Combustion Chamber; BBBS, BB0S, B00S and 000S. It can be seen in the figure that all the four cases are producing qualitatively consistent results. In all four cases, no matter the investigation is experimental, URANS or LES, the trend of the over-pressure phenomenon suggests the presence of three main consecutive stages. The first stage shows a pressure increase with a low rate. This is followed by the second stage where the rate of increase of pressure is suddenly increased to a much higher rate shooting the pressure to its peak value. This leads to the last stage where the pressure starts to decay.

In all four cases, the URANS predictions over-estimates the time needed to reach the peak pressure by about 50%. There is no consistency in the level of agreement between the value of the peak pressure obtained by URANS and that of the experimental and LES calculations which are much closer to each other.

Though the agreement with experiments is much better for the LES calculations, there are still some discrepancies whether in a slight lag in the early quasi-laminar stage or in the ability to reproduce exact peak pressure value especially in the 000S case which is featured by the least level of turbulence amongst the

four considered cases. Same points are revealed when comparing the flame position change with time shown in the same figure. The flame position history is revealing similar features to that of the over-pressure except for an impressive agreement between experimental and LES results for cases with higher turbulence levels. The discrepancies are evident in all URANS cases and the case with less turbulence, ie the '000S' case also the LES fails to represent the experimental results adequately.

Figure 5 shows a comparison of the sequence of experimental images showing the flame structure after ignition as obtained from [7] and numerical snapshots for reaction contours calculated by [9] to our present URANS calculations for the BBBS configuration. It is again showing the qualitative agreement between the three sets of results regarding the response of the flow to impinging with either the baffles or the box, but much less in value and later in time reaction rates are obtained for the URANS calculations.

Figure 6 shows contours of the reaction rate as been calculated by URANS method for the three configurations 'BB0S', 'B00S' and '000S' starting from 3ms, 4 ms, 5 ms, 5.4 ms, 5.8 ms, 6.2 ms, 6.6 ms, 7 ms, 7.4 ms, 7.8 ms, 8.2 ms, 8.6 ms and 9 ms. It is shown that the reaction rate decreases with the decrease of turbulence level and thus the reaction takes longer time. This obviously is longer than what would be expected in both the experimental measurements and LES calculations.

## CONCLUDING REMARKS

This study shows a comparison between simulations of hydrogen combustion conducted with two different modeling approaches, namely the URANS and LES. Both techniques successfully reproduces the qualitative features as observed by the experimental measurements. However, details of flame position and overpressure changes with time, values of peak pressure reached and time taken from ignition until reaching the peak pressure was only reasonable for LES calculations in conditions where turbulence levels attained due to impingement with blockages were sufficiently high. Both techniques do not conform the quasi-laminar case were the only blockage present in the geometrical configuration was a box in the middle of the chamber. This is attributed to the laminar case and it ought not to be simulated by any turbulence model neither RANS nor LES.

## NOMENCLATURE

| | |
|---|---|
| $Cij$ | Cross stress, |
| $C$ | Reaction progress variable |
| $C_1$ | Model coefficient in Smagorinsky model |
| $C_2$ | Model coefficient in Smagorinsky model |
| $C_s$ | Smagorinsky coefficient |
| $h$ | Enthalpy, $kJ/kg$ |
| $K$ | turbulent kinetic energy |
| $Ka$ | Karlovitz number |
| $L_{ij}$ | Leonard stress, $(m/s)^2$ |
| $L_y$ | Length scale of wrinkle flame front, $m$ |
| $l$ | Length scale, $m$ |
| $p$ | Pressure, kPa |
| $q_c$ | Chemical source term, $kJ/kg$ |
| $S$ | Stress tensor, $(m/s)^2$ |
| $S_{ij}$ | Strain rate, $s^{-1}$ |
| $T$ | Temperature, $K$ |
| $T_{ij}$ | Sub-test-scale stress tensor, $(m/s)^2$ |
| $t$ | Time, $s$ |
| $u$ | Velocity in x-direction, $m/s$ |
| $u'$ | RMS fluctuations, $m/s$ |
| $Y_{fu}$ | Fuel mass fraction |
| $Y_{fu}^0$ | Fuel mass fraction in un-burnt mixture |

### Greek Symbols

| | |
|---|---|
| $\alpha_1$ | Model constant |
| $\alpha_3$ | Model constant |
| $\alpha_{ij}$ | Traceless tensor, $(m/s)^2$ |
| $\beta$ | Model coefficient simple FSD equation |
| $\beta_1$ | Model constant |
| $\beta_3$ | Model constant |
| $\beta_{ij}$ | Traceless tensor, $(m/s)^2$ |
| $\mu$ | Dynamic viscosity, $kg/m.s$ |
| $\dot{\omega}_c$ | Chemical reaction rate, $kg/s$ |
| $\varepsilon$ | Turbulent kinetic energy, $kJ/kg$ |
| $\rho$ | Fluid density, $kg/m^3$ |

| | |
|---|---|
| $\rho_u$ | Unburned gas density, $kg/m^3$ |
| $\delta_{ij}$ | Kronecker delta |
| $\delta_L$ | Flame thickness, $m$ |
| $\delta_c$ | Lower cut-off scale, $m$ |
| $\tau_{ij}^{sgs}$ | Residual stress, $(m/s)^2$ |
| $\bar{\Delta}$ | Filter width, $m$ |
| $\Lambda$ | Unresolved flame surface density at test filter, $m^{-1}$ |

Subscript/Superscript

| | |
|---|---|
| $fu$ | fuel |
| K | Kolmogrov |
| u | Unburnt |
| K | |

**REFERENCES**


[1] FLUENT, "A Theorey Guide," *Canonsbg. P. A. ANSYS Inc.*, 2016.

[2] R. W. Bilger, S. B. Pope, K. N. C. Bray, and J. F. Driscoll, "Paradigms in turbulent combustion research," *Proc. Combust. Inst.*, vol. 30, no. 1, pp. 21–42, 2006.

[3] N. Peters, *Turbulent Combustion*. Cambridge University Press, 2000.

[4] V. Zimont, "Gas premixed combustion at high turbulence, Turbulence Flame Closure Model," *Exp. Therm. Fluid Sci.*, vol. 21, pp. 179–186, 2000.

[5] C. Meneveau and T. Poinsot, "Stretching and quenching of flamelets in premixed turbulent combustion," *Combust. Flame*, 1991.

[6] O. Colin, F. Ducros, D. Veynante, T. Poinsot, and O. Colin, "A thickened flame model for large eddy simulations of turbulent premixed combustion A thickened flame model for large eddy simulations of turbulent premixed combustion," vol. 1843, no. 2000, 2012.

[7] A. R. Masri, A. Alharbi, S. Meares, and S. S. Ibrahim, "A comparative study of turbulent premixed flames propagating past repeated obstacles," *Ind. Eng. Chem. Res.*, 2012.

[8] M. A. Abdel-Raheem, S. S. Ibrahim, and W. Malalasekera, "Numerical Experiments of Hydrogen-Air Premixed Flames," *Int. J. Res. Eng. Sci. ISSN (Online*, pp. 2320–9364, 2014.

[9] M. A. Abdel-Raheem, S. S. Ibrahim, W. Malalasekera, and A. R. Masri, "Large Eddy simulation of hydrogen-air premixed flames in a small scale combustion chamber," *Int. J. Hydrogen Energy*, 2015.

[10] H. Xiao, Q. Wang, X. He, J. Sun, and X. Shen, "Experimental study on the behaviors and shape changes of premixed hydrogen e air flames propagating in horizontal duct," *Int. J. Hydrogen Energy*, vol. 36, no. 10, pp. 6325–6336, 2011.

[11] V. N. Gamezo, T. Ogawa, and E. S. Oran, "Flame acceleration and DDT in channels with obstacles : Effect of obstacle spacing," *Combust. Flame*, vol. 155, no. 1–2, pp. 302–315, 2008.

[12] P. Quillatre, P., Vermorel, O., Poinsot, T. and Ricoux, "Large Eddy Simulation of Vented De fl agration," *Ind. Eng. Chem. Res.*, 2013.

[13] O. Vermorel, P. Quillatre, and T. Poinsot, "LES of explosions in venting chamber : A test case for premixed turbulent combustion models," vol. 183, pp. 207–223, 2017.

[14] M. Fairweather, G. K. Hargrave, S. S. Ibrahim, and D. G. Walker, "Studies of Premixed Flame Propagation in Explosion Tubes," vol. 518, pp. 504–518, 1999.

[15] S. N. D. H. Patel, S. S. Ibrahim, and M. A. Yehia, "Flamelet surface density modelling of turbulent deflagrating flames in vented explosions," *J. Loss Prev. Process Ind.*, 2003.

[16] S. S. Ibrahim and A. R. Masri, “The effects of obstructions on overpressure resulting from premixed flame deflagration,” vol. 14, no. 2001, pp. 213–221, 2006.

[17] A. R. Masri, S. S. Ibrahim, and B. J. Cadwallader, “Measurements and large eddy simulation of propagating premixed flames,” vol. 30, pp. 687–702, 2006.

[18] S. S. Ibrahim, S. R. Gubba, A. R. Masri, and W. Malalasekera, “Calculations of explosion deflagrating flames using a dynamic flame surface density model,” *J. Loss Prev. Process Ind.*, 2009.

[19] S. S. Ibrahim, S. Rao Gubba, and W. Malalasekera, “A Parametric Study on Large Eddy Simulations of Turbulent Premixed Flames.”

[20] J. E. (1979): A. theoretical analysis of nitric oxide production in a methane-air turbulent diffusion flame. E. T. R. Marble, F. E., Broadwell, “No Title.”

[21] S. R. Gubba, S. S. Ibrahim, W. Malalasekera, and A. R. Masri, “LES modeling of premixed deflagrating flames in a small-scale vented explosion chamber with a series of solid obstructions,” in *Combustion Science and Technology*, 2008.

[22] S. R. Gubba, S. S. Ibrahim, W. Malalasekera, and A. R. Masri, “An assessment of large eddy simulations of premixed flames propagating past repeated obstacles,” *Combust. Theory Model.*, 2009.

[23] R. Knikker, D. Veynante, and C. Meneveau, “A dynamic flame surface density model for large eddy simulation of turbulent premixed combustion,” vol. 91, no. 2004, 2011.

[24] S. R. Gubba, S. S. Ibrahim, and W. Malalasekera, “Dynamic flame surface density modelling of flame deflagration in vented explosion,” *Combust. Explos. Shock Waves*, 2012.

[25] M. A. Abdel-Raheem, S. S. Ibrahim, W. Malalasekera, and A. R. Masri, “LARGE EDDY SIMULATION OF HYDROGEN-AIR PROPAGATING FLAMES,” pp. 8–13, 2013.

[26] A. R. Masri, S. S. Ibrahim, N. Nehzat, and A. R. Green, “Experimental study of premixed flame propagation over various solid obstructions,” *Exp. Therm. Fluid Sci.*, 2000.

[27] D. B. Launder, B. E. and Spalding, “The numerical computation of turbulent flows,” *Comput. Methods Appl. Mech. Eng.*, vol. 3, no. 2, pp. 269–289, 1974.

[28] S. Smagorinsky, “GENERAL CIRCULATION EXPERIMENTS WITH THE PRIMITIVE EQUATIONS I. THE BASIC EXPERIMENT*,” 1963.

[29] Yehia, M. A., Ibrahim, S. S. and Haridy, H. K., “Numerical study of LPG premixed combustion thermodynamics effects,” in *Thirteenth International Conference of Fluid Dynamics*, 2018, pp. ICFD13-EG-6074.

[30] M. Germano *et al.*, “A dynamic subgrid - scale eddy viscosity model A dynamic subgrid-scale eddy viscosity model,” vol. 1760, no. 1991, 2015.

[31] S. Gubba, S. Ibrahim, and W. Malalasekera SSIbrahim, “LES STUDY OF INFLUENCE OF OBSTACLES ON TURBULENT PREMIXED FLAMES IN A SMALL SCALE VENTED CHAMBERS.”

[32] D. Sathiah, P., Komen, E. and Roekaerts, “The role of CFD combustion modelling in hydrogen safety management - part 1: validation based on small scale experiments.,” *Nucl Eng Des*, vol. 248, pp. 93–107, 2012.

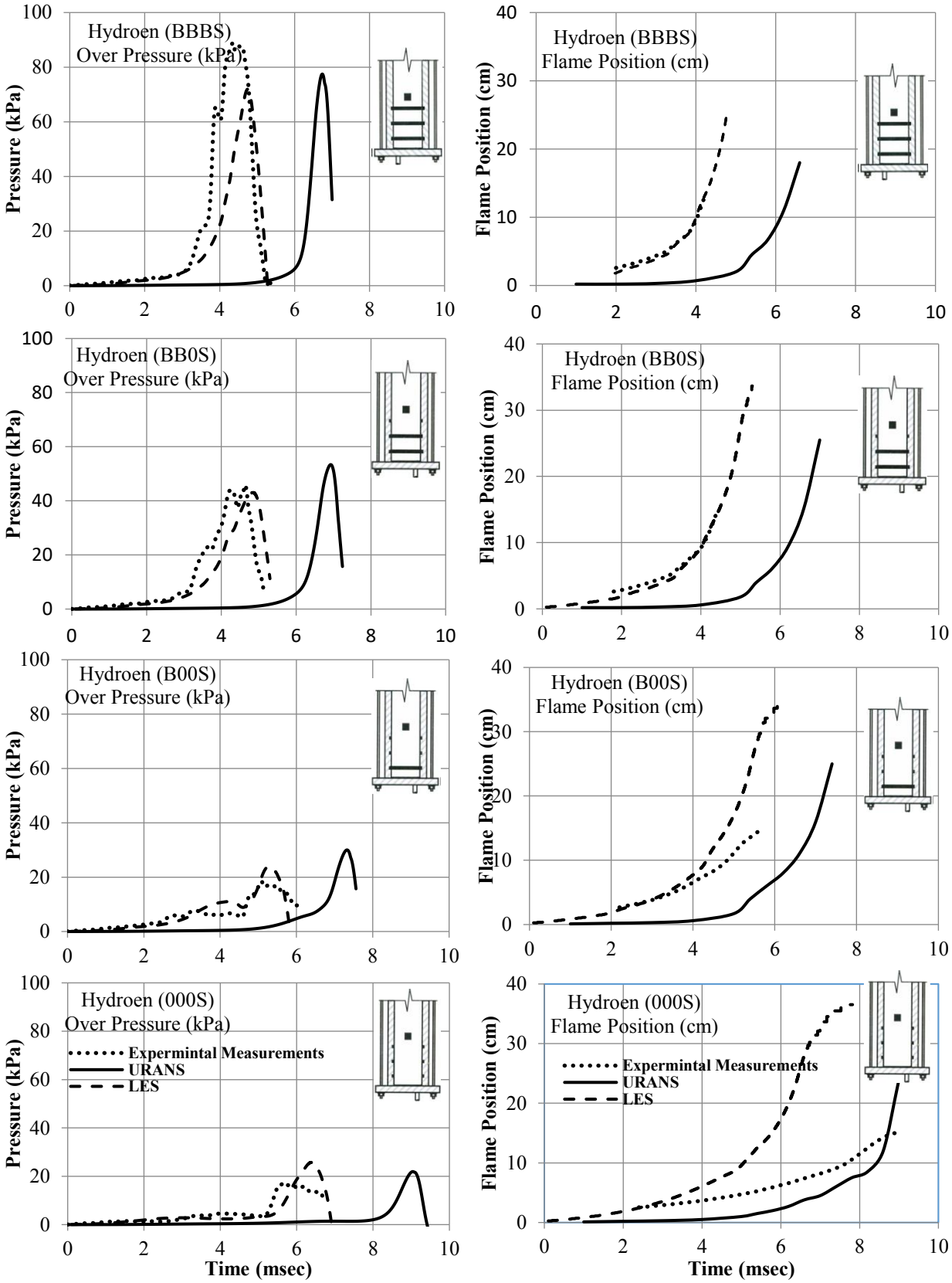


Figure 4: Comparison between URANS, LES and experimental results [7] for overpressure and flame position time traces of Hydrogen premixed flames flowing through four different burner configurations BBBS, BB0S, B00S and 000S.

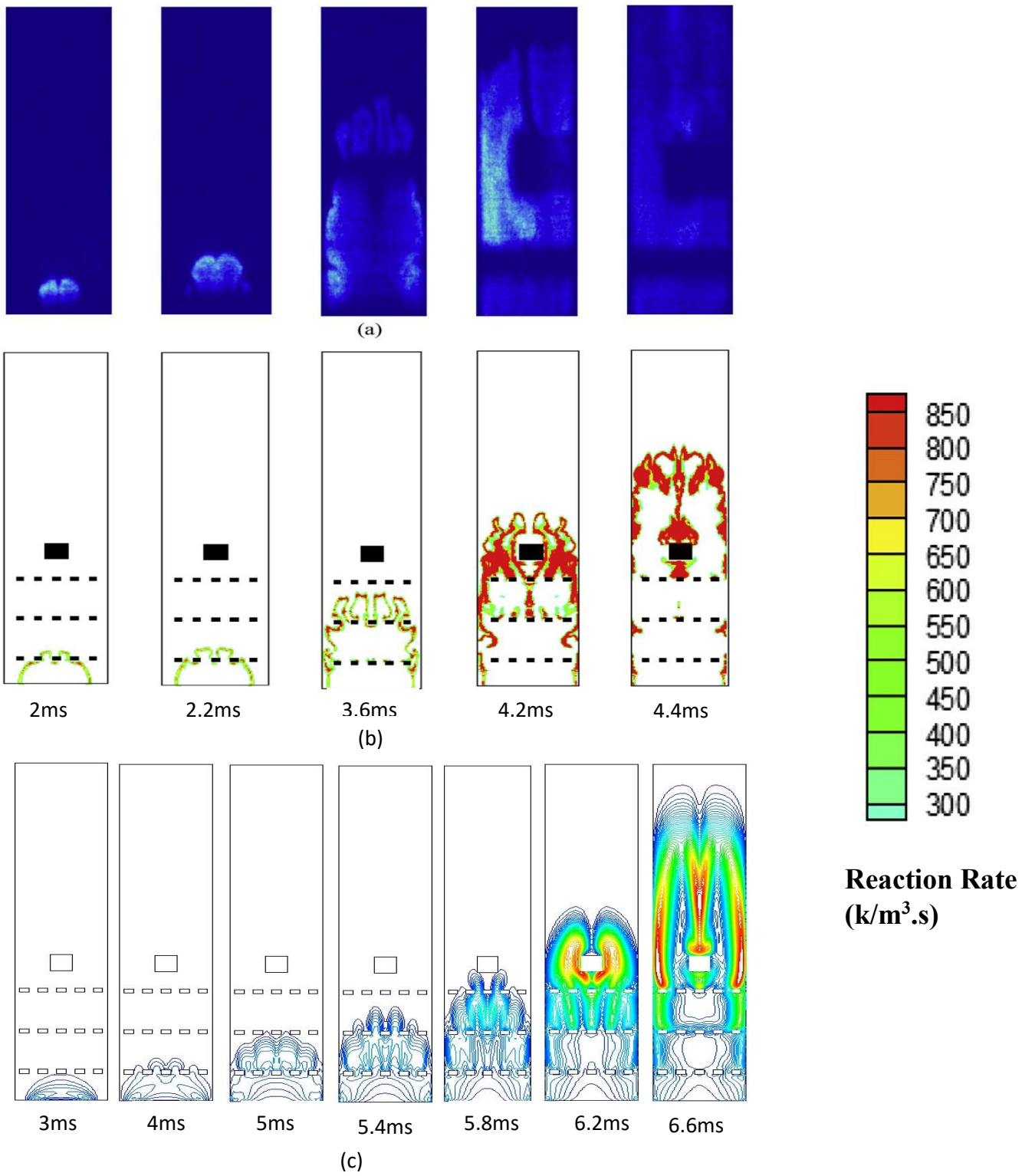


Fig.5 Comparison between sequence of images showing flame structure after ignition. (a) LIF-OH images from experiments [7]. (b) Numerical snapshots for reaction rate contours [9]. (c) URANS reaction rate cotours.